International Journal of Environmental Sciences
ISSN: 2229-7359
Vol. 11 No. 19s, 2025
https://www.theaspd.com/ijes.php

Design Of High Step-Up DC - DC Converter For Renewable Energy Systems

[1]Dr.K.Radha Lakshmi, [2]M.Pushpalatha, [3] R. Amutha,[4]Dr.S.Nagarajan

[1]Assistant Professor(SG)/Department of Electrical and Electronics Engineering
Solamalai College of Engineering,Madurai
[2]Assistant professor, Department of Electrical and Electronics Engineering, ULTRA College of Engineering, Madurai.
[3]Assistant professor,Department of Electrical and Electronics Engineering, ULTRA College of Engineering, Madurai.
[4]Professor/Department of Electrical and Electronics Engineering
Solamalai College of Engineering,Madurai

ABSTRACT

In this paper, a high step-up converter using coupled inductor with Fuzzy Logic Control is analyzed and simulated. The converter uses a coupled inductor and a switched capacitor circuit to achieve high voltage conversion ratio. Two capacitors and diodes constitute the switched capacitor circuit. The two capacitors are charged in parallel during the switch-off period and are discharged in series during the switch-on period by the energy stored in the coupled inductor to achieve a high step-up voltage gain. Switch voltage stress and the circulating current are reduced by a clamp circuit which is composed of a diode followed by a capacitor. Thus the efficiency of the converter is improved. The operating principle and the steady state analysis are discussed in detail. A Fuzzy logic controller is designed such that it eliminates the Voltage Drift problem.

INDEX TERMS—Coupled Inductor, FLC, Switched Capacitor circuit.

INTRODUCTION

Renewable energy sources (RES) have experienced a fast development in recent years. These systems employ with micro sources like PV, fuel cells etc. Though PV cells can be made into array and connected in series to produce high voltage there exist serious problems like shadowing effects, short circuit which drastically reduces its efficiency. In order to overcome such adverse effects this micro source energy is utilized by the high step up converter to produce high voltage and satisfy the demands. Conventional boost converters can't provide such a high DC voltage gain for extreme duty cycle.

Thus high step up dc-dc converters are used as front end converters to step from low voltage to high voltage which are required to have a large conversion ratio, high efficiency and small volume [1].In some converters active clamp circuit is used to overcome voltage spikes caused by the leakage inductance of the coupled inductor. Though ZVS technique is employed for soft switching it can't sustain light loads [2].Different switching structures are formed either two capacitor or two inductor with two- three diodes. Both the step up and step down operations can be performed in this topology, Performance of hybrid converters are better than classical converters but still its costlier to implement [3]. Low level voltage from the PV, fuel cells is connected to Kilo watt level using step up dc- dc converter and inverter circuits. Voltage spikes and switching losses are eliminated by active clamping. In dc-ac, inverter always tends to draw ac ripple current at twice the output frequency. Resonant inductors cost and circuit volume is high [4]. In some converters high voltage conversion is obtained by changing transformer turns ratio which will increase the overall efficiency but still the operation of main switch involves hard switching and also EMI noise gets raised [5]. Impacts of SiC (silicon carbide) MOSFETS on converter, switching and conduction losses are reduced even though fast switching is done. Si diodes have ideal, but sill SiC devices processes large

amount of ringing current at turn OFF relatively to other devices. Package of external diode and the diode itself have more parasitic capacitances that are added to the devices parasitic aggravating the ringing [6].Here, the voltage step is done without a transformer and a high voltage gain s achieved without an extremely high duty ratio but still the circuit becomes more bulky as more number of passive components are used [7]. Though this converter provides a non-pulsating current by using an auto transformer, duty ratio is limited by 0.5 and not suitable for non-linear loads [8].Here voltage stress of the active switch is reduced thereby the conversion efficiency is improved. This converter requires a multi winding transformer which makes the circuit design complex [9].

This converter avoids extremely narrow turn off period, ripples and switching losses are eliminated by ZVS technique. It uses two coupled inductors which makes the circuit complex [10]. In this converter no additional magnetic components used, switching losses are minimized by adopting a regenerative snubber circuit. As the circuit uses more switches controlling is complex [11]. In this converter high voltage gain is obtained but the circuit has more passive components [12]. It employees single ended scheme cost is reduced. Galvanic isolation is needed, but suitable only for low power and frequency applications [13], [14]. In this converter no need of extreme duty ratio but if conduction losses or switching losses occurs the efficiency is reduced [15].

It is possible to generate the non-isolated dc-dc converters but the major drawback is that switching frequency must be maintained constant and the turn ratio of the auto transformer must be unity [16]. Some converters operate at very high frequency with fast transient response. The main switch is fabricated from an integrated power process, the layouts can be changed to vary the parasitic, however design of switch layout is complex, fixed frequency and constant duty ratio must be maintained [17]. This converter provides high voltage gain and can be employed for high power applications however the duty ratio is limited to 0.85 [18], [19]. In this, the energy of the leakage inductor is recycled to the output load directly, limiting the voltage spike on the main switch. To achieve a high step-up gain, it has been proposed that the secondary side of the coupled inductor can be used as flyback and forward converters [20], [21].In some converters voltage gain is improved through output voltage stacking [22].

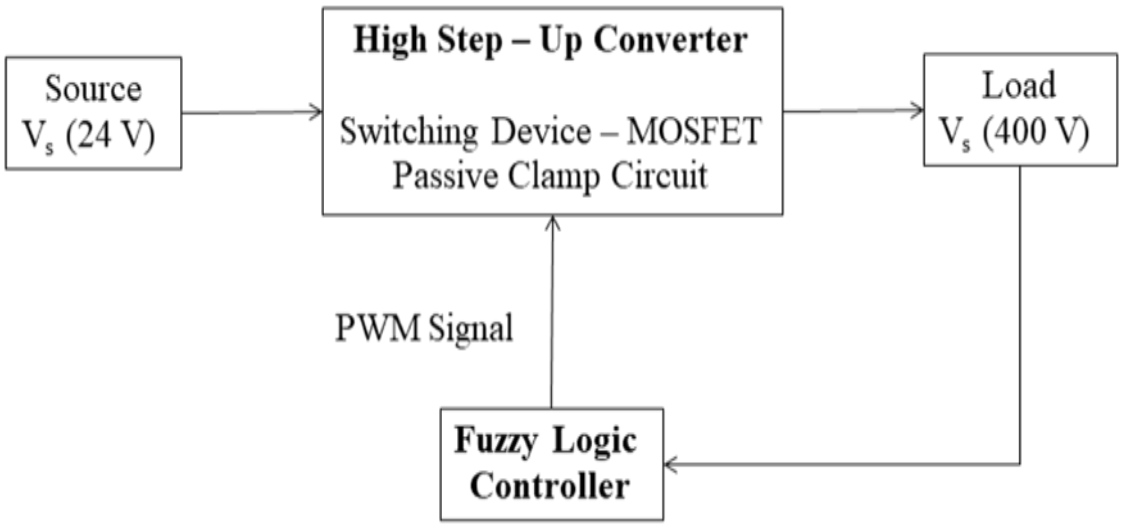

Fig. 1 Block Diagram.

The main objective is to improve the Voltage Gain of the Step-up Converter and also to reduce Voltage stress of the circuit. Further the Voltage Drift problem is reduced using closed loop control of the proposed converter with fuzzy logic controller. From Fig.1, The output voltage from the converter is fed as feed back to the FLC; there it compares the feedback voltage signal and the reference voltage signal to produce PWM pulse which triggers the

main switch of the converter.

The output voltage from the converter is fed as feed back to the Controller; there it compares the feedback voltage signal and the reference voltage signal to produce PWM pulse which triggers the main switch of the converter.

II. OPERATING PRINCIPLE OF THE PROPOSED CONVERTER

Fig .2 shows the circuit topology of the proposed converter, which is composed of dc input voltage V_{in} , main switch S, coupled inductors N_p and N_s , one clamp diode D_1 , clamp capacitor C_1, two capacitors C_2 and C_3, two diodes D_2 and D_3, output diode D_o, and output capacitor C_o. The equivalent circuit model of the coupled inductor includes magnetizing inductor L_m, leakage inductor L_k, and an ideal transformer.

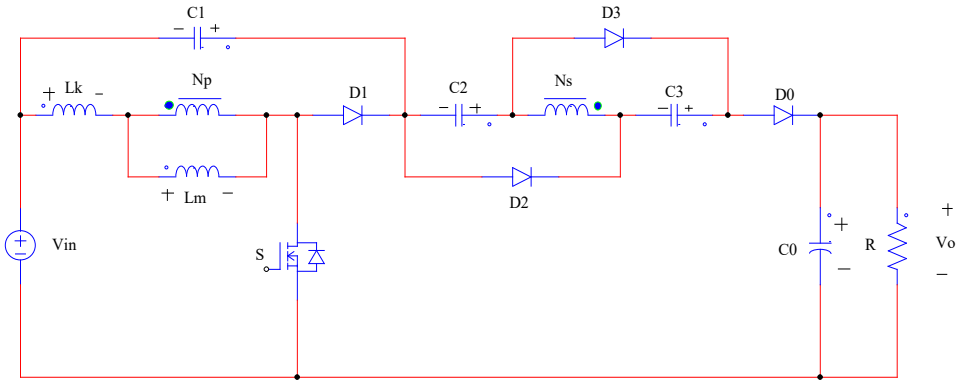

Fig.2 Circuit Configuration of the Proposed Converter.

The leakage- inductor energy of the coupled inductor is recycled to capacitor C_1, and thus, the voltage across the switch S can be clamped. The voltage stress on the switch is reduced significantly. Thus, low conducting resistance RDS (ON) of the switch can be used. Based on the topology, the proposed converter combines the concept of switched-capacitor and coupled-inductor techniques.

The switched-capacitor technique in is that capacitors can be parallel charged and series discharged to achieve a high step-up gain. Based on the concept, the proposed converter puts capacitors C_2 and C_3 on the secondary side of the coupled inductor. Thus, capacitors C_2 and C_3 are charged in parallel and are discharged in series by the secondary side of the coupled inductor when the switch is turned off and turned on. Because the voltage across the capacitors can be adjusted by the turn ratio, the high step-up gain can be achieved significantly. Also, the voltage stress of the switch can be reduced. The parallel-charged current is not inrush. Thus, the proposed converter has low conduction loss.

Moreover, the secondary-side leakage inductor of the coupled inductor can alleviate the reverse-recovery problem of diodes, and the loss can be reduced. In addition, the proposed converter adds capacitors C_2 and C_3 to achieve a high step-up gain without an additional winding stage of the coupled inductor. The coil is less than that of other coupled inductor converters. The main operating principle is that, when the switch is turned on, the coupled-inductor-induced voltage on the secondary side and magnetic inductor L_m is charged by V_{in}. The induced voltage makes V_{in}, V_{C1}, V_{C2}, and V_{C3} release energy to the output in series. Fig. 3 shows the typical waveforms.

International Journal of Environmental Sciences
ISSN: 2229-7359
Vol. 11 No. 19s, 2025
https://www.theaspd.com/ijes.php

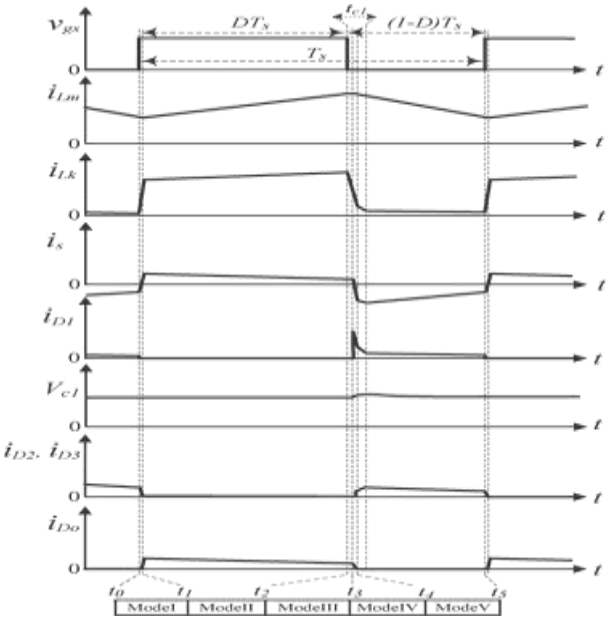

To simplify the circuit analysis, the following conditions are assumed.

1) Capacitors C_1, C_2, C_3, and C_o is large enough. Thus, V_{C1}, V_{C2}, V_{C3}, and V_0 are considered as constants in one switching period.

2) The power devices are ideal, but the parasitic capacitor of the power switch is considered.

3) The coupling coefficient of the coupled inductor k is equal to $L_m / (L_m+L_k)$ and the turn ratio of the coupled inductor n is equal to N_s / N_p.

A. Mode of Operation

This section presents the operation principle of the proposed converter. There are five operating modes in one switching period. The current-flow path of each mode of the circuit is shown.

a)Mode I [t_0- t_1]

During this time interval, S is turned on. Diodes D_1 and D_o are turned off, and D_2 and D_3 are turned on. The current-flow path is shown in Fig.4 (a).The voltage equation on the leakage and magnetic inductors of the coupled inductor on the primary side is expressed as $V_{in} = V_{Lk} + V_{Lm}$. The leakage inductor L_k starts to charge by V_{in}. Due to the leakage inductor L_k, the secondary-side current is of the coupled inductor is decreased linearly. Output capacitor C_o provides its energy to load R. When current i_{D2} becomes zero at $t = t_1$, this operating mode ends.

b)Mode II [t_1- t_2]

During this time interval, S remains turned on. Diodes D_1, D_2, and D_3 are turned off and D_o is turned on. The current-flow path is shown in Fig.4 (b). Magnetizing inductor L_m stores energy generated by dc- source V_{in}. Some of the energy of dc-source V_{in} transfers to the secondary side via the coupled inductor. Thus, the induced voltage V_{L2} on the secondary side of the coupled inductor makes V_{in}, V_{C1}, V_{C2}, and V_{C3}, which are connected in series, discharge to high-voltage output capacitor Co and load R. This operating mode ends when switch S is turned off at $t = t_2$.

C) Mode III [t_2- t_3]

During this time interval, S is turned off. Diodes D_1, D_2, and D_3 are turned off and D_o is turned on. The current-

International Journal of Environmental Sciences
ISSN: 2229-7359
Vol. 11 No. 19s, 2025
https://www.theaspd.com/ijes.php

flow path is shown in Fig.4© The energies of leakage inductor L_k and magnetizing inductor L_m charge the parasitic capacitor C_{ds} of main switch S. Output capacitor C_0 provides its energy to load R. When the capacitor voltage V_{C1} is equal to $V_{in} + V_{ds}$ at $t = t_3$, diode D_1 conducts, and this operating mode ends.

d)Mode IV [t_3-t_4]

During this time interval, S is turned off. Diodes D_1 and D_o are turned on, and D_2 and D_3 are turned off. The current-flow path is shown in Fig.4(d). The energies of leakage inductor L_k and magnetizing inductor L_m charge clamp capacitor C_1. The energy of leakage inductor L_k is recycled. Current i_{lk} decreases quickly. Secondary-side voltage V_{L2} of the coupled inductor continues charging high-voltage output capacitor C_o and load R in series until the secondary current of the coupled inductor is equal to zero. Meanwhile, diodes D_2 and D_3 start to turn on. When i_{Do} is equal to zero at $t = t_4$, this operating mode ends.

e) Mode V [t_4-t_5]

During this time interval, S is turned off. Diodes D_1, D_2, and D_3 are turned on and D_o is turned off. The current-flow path is shown in Fig. 4 (e) Output capacitor C_o is discharged to load R. The energies of leakage inductor L_k and magnetizing inductor L_m charge the clamp capacitor C_1. Magnetizing inductor L_m is released via the secondary side of the coupled inductor and charges capacitors C_2 and C_3. Thus, capacitors C_2 and C_3 are charged in parallel. As the energy of leakage inductor L_k charges capacitor C_1, the current i_{lk} Decreases and i_s increases gradually. This mode ends at $t = t_6$ when S is turned on at the beginning of the next switching period.

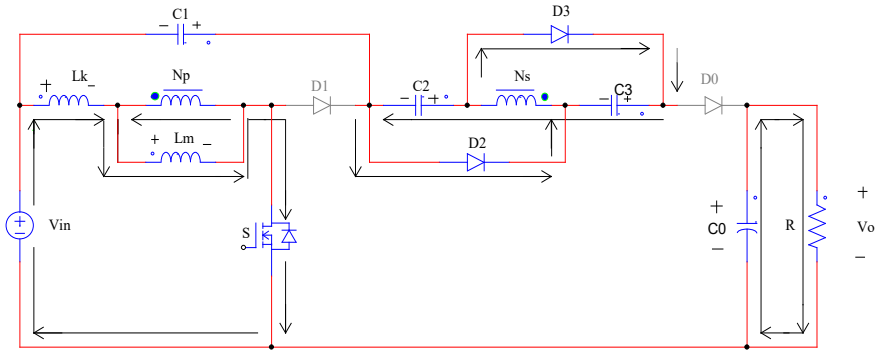

a) Mode I [t_0.t_1].

International Journal of Environmental Sciences
ISSN: 2229-7359
Vol. 11 No. 19s, 2025
https://www.theaspd.com/ijes.php

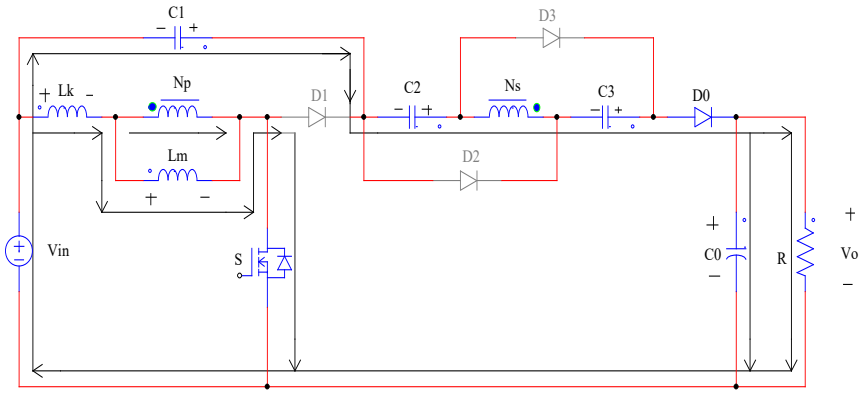

b) Mode II [t_1-t_2].

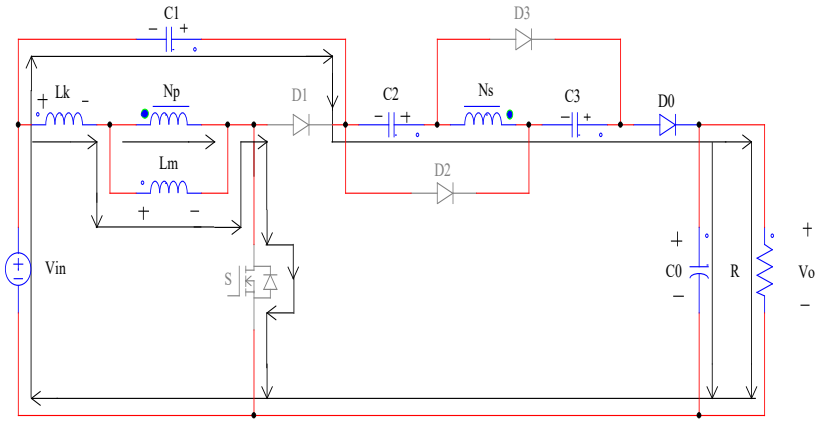

C)Mode III [t_2-t_3].

International Journal of Environmental Sciences
ISSN: 2229-7359
Vol. 11 No. 19s, 2025
https://www.theaspd.com/ijes.php

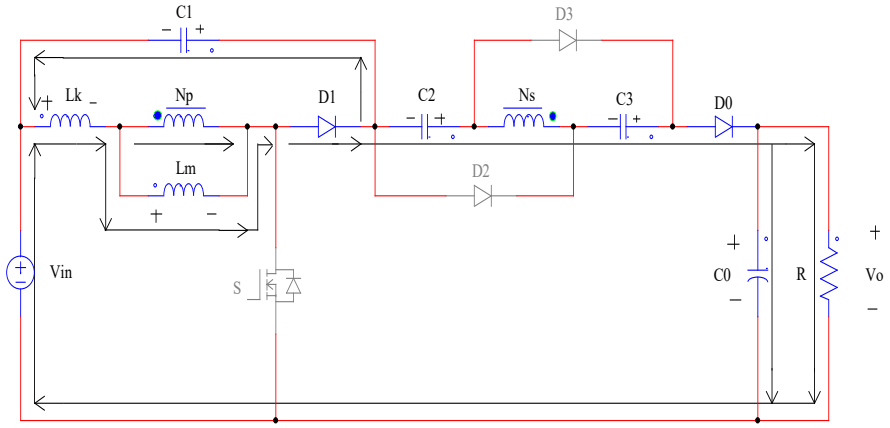

d) Mode IV [t_3-t_4].

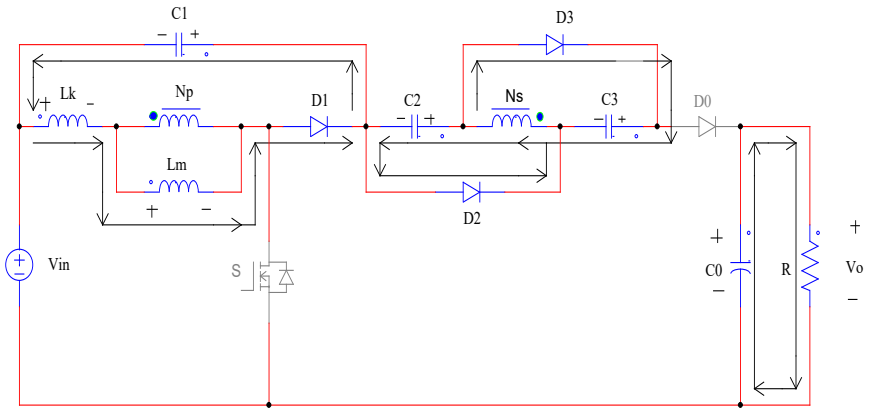

e) Mode V [t_4- t_5].

Fig. 4 Operating Modes.

III Analysis of the Proposed Converter

According to [1], the energy stored in the leakage inductor L_k of the coupled inductor is released to capacitor C_1. The energy-released duty cycle D_{c1} can be expressed as

$$D_{C1} = \frac{t_{c1}}{T_s} = \frac{2(1-D)}{n+1} \quad (1)$$

The equivalent circuit and state definition of the newly designed converter is depicted in Fig.2, where the

transformer is modeled as an ideal transformer. The turn ratio of this ideal transformer is defined as

$$n = \frac{N_2}{N_1} \quad (2)$$

From Fig 4.b),

$$V_{L1}^{ON} = \frac{L_m}{L_m + L_{k1}} V_{in} = KV_{in} \quad (3)$$

$$V_{L2}^{ON} = nV_{L1}^{ON} = nKV_{in} \quad (4)$$

$$V_0 = V_{in} + V_{C1} + V_{C2} + V_{L2}^{ON} + V_{C3} \quad (5)$$

By Voltage Second Balance principle,

$$\int_0^{DT_S} V_{L1}^{ON} dt + \int_{DT_S}^{T_S} V_{L1}^{OFF} dt = 0 \quad (6)$$

$$\int_0^{DT_S} V_{L2}^{ON} dt + \int_{DT_S}^{T_S} V_{L2}^{OFF} dt = 0 \quad (7)$$

By solving (6), (7), we get,

$$V_{L1}^{OFF} = \frac{-Dk}{1-D} V_{in} \quad (8)$$

$$V_{L2}^{OFF} = \frac{-nDk}{1-D} V_{in} \quad (9)$$

As the capacitors are charged during switch OFF mode, the voltage across the capacitors can be obtained from fig.3.4,

$$V_{C1} = \frac{D}{1-D} . V_{in} . \frac{(1+k)+(1-k)}{2} \quad (10)$$

$$V_{C2} = V_{C3} = -V_{L2}^{ON}$$

$$= \frac{nDk}{1-D} V_{in} \quad (11)$$

International Journal of Environmental Sciences
ISSN: 2229-7359
Vol. 11 No. 19s, 2025
https://www.theaspd.com/ijes.php

Substituting (4), (10), (11) in (5), we get,

$$V_0 = \frac{1+nk}{1-D}.V_{in} + \frac{D}{1-D}.\frac{(k-1)+n(1+k)}{2}.V_{in} \quad (12)$$

$$\frac{V_0}{V_{in}} = \frac{1+nk}{1-D} + \frac{D}{1-D}.\frac{(k-1)+n(1+k)}{2} \quad (13)$$

According to the description of operating modes, voltage stresses on active switch S and diodes D_1, D_2, D_3, and D_o are given as

$$V_{ds} = \frac{1}{1-D}V_{in} = \frac{V_0+nV_{in}}{2n+1} \quad (14)$$

$$V_{D1} = \frac{1}{1-D}V_{in} = \frac{V_0+nV_{in}}{2n+1} \quad (15)$$

$$V_{D2} = V_{D3} = V_{D0} = \frac{n}{1-D}V_{in}$$

$$= \frac{n(V_0+nV_{in})}{2n+1} \quad (16)$$

Equations (14)–(16) mean that, under the same voltage ratio, the voltage stresses can be adjusted by the turn ratio of the coupled inductor.

IV Designing of Parameters

Let:

Input Voltage V_{in}= 24 V

Output Power P_0= 200 W

Switching Frequency f = 50 KHz

Load Resistance R = 800Ω

A. Design of Coupled Inductor

$$k = \frac{L_m}{L_m+L_k} \quad (17)$$

$$\Delta I_1 = \frac{DkV_{in}}{L_1 f(2D-1)} \quad (18)$$

$$\Delta I_2 = \frac{nDkV_{in}}{L_2 f(2D-1)} \quad (19)$$

From equation (13), (17) - (19) select the values L1 =1.48mH, L_2 = 5.62 mH. Here the L_m& L_k values are chosen

as 48μH & 0.25μH.

B.Selection of Switching Device

MOSFET:

It is chosen as switch as it is cost effective, high commutation speed, low on state resistance, improved gate and high speed power switching.

IV. FUZZY LOGIC CONTROLLER DESIGN

The block diagram of fuzzy logic controller (FLC) is shown in fig.5. It consists of three main blocks: fuzzification, inference engine and defuzzification. The two FLC input variables are the error E and change in error E*. Depending on membership functions and the rules FLC operates.

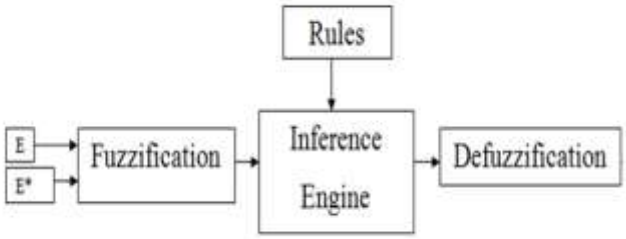

Fig.5 Block Diagram of FLC.

A. Fuzzification

The membership function values are assigned to the linguistic variables using seventeen fuzzy subsets. Table-I shows the rules of FLC. E and E* are input variables, where E is the error between the reference and actual voltage of the system, E* is the change in error in the sampling interval.

B. Inference Engine

Mamdani method is used with Max-Min operation fuzzy combination. Fuzzy inference is based on fuzzy rules. Rules are framed in inference engine block. The output membership function of each rule is given by MIN (Minimum) operator and MAX (Maximum) operator.

C. Defuzzification

The output of fuzzy controller is a fuzzy subset. As the actual system requires a non fuzzy value of Control, defuzzication is required. Defuzzifier is used to convert the linguistic fuzzy sets back into actual value. The membership functions of error (E), change in error (E*) and Duty ratio (D) are shown in fig. 6, 7, 8.Fig.9 shows the representation of the typical Rule Surface of fuzzy logic controller.

International Journal of Environmental Sciences
ISSN: 2229-7359
Vol. 11 No. 19s, 2025
https://www.theaspd.com/ijes.php

TABLE-I RULE TABLE FOR FLC

E* / E	N	Z	P
N8	N7	N8	N6
N7	N6	N7	N8
N6	N5	N6	N7
N5	N4	N5	N6
N4	N3	N4	N5
N3	N2	N3	N4
N2	N8	N2	N3
N1	N8	Z	P2
Z	P1	Z	N1
P1	P2	P1	Z
P2	P3	P2	P1
P3	P4	P3	P1
P4	P3	P4	P3
P5	P6	P5	P5
P6	P7	P6	P5
P7	P8	P7	P6
P8	P8	P8	P7

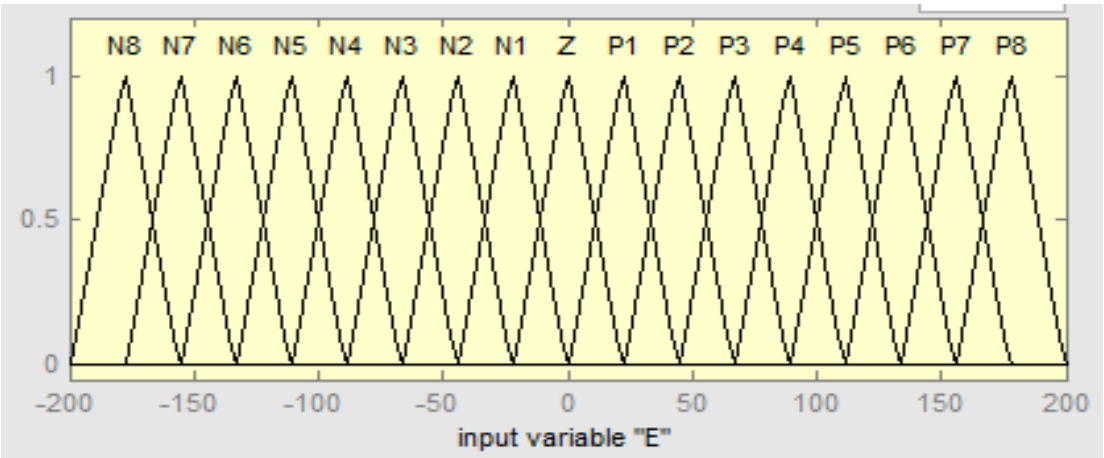

Fig.6 Membership Functions of Error (E).

International Journal of Environmental Sciences
ISSN: 2229-7359
Vol. 11 No. 19s, 2025
https://www.theaspd.com/ijes.php

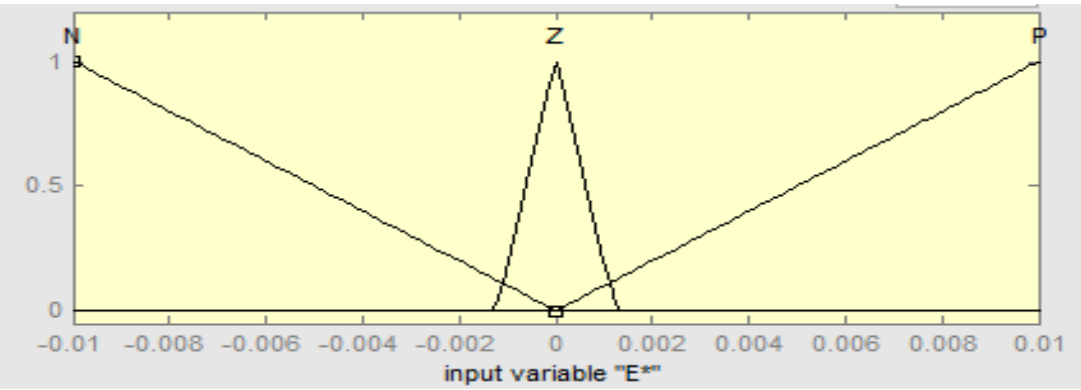

Fig.7 Membership Functions of Change in Error (E*).

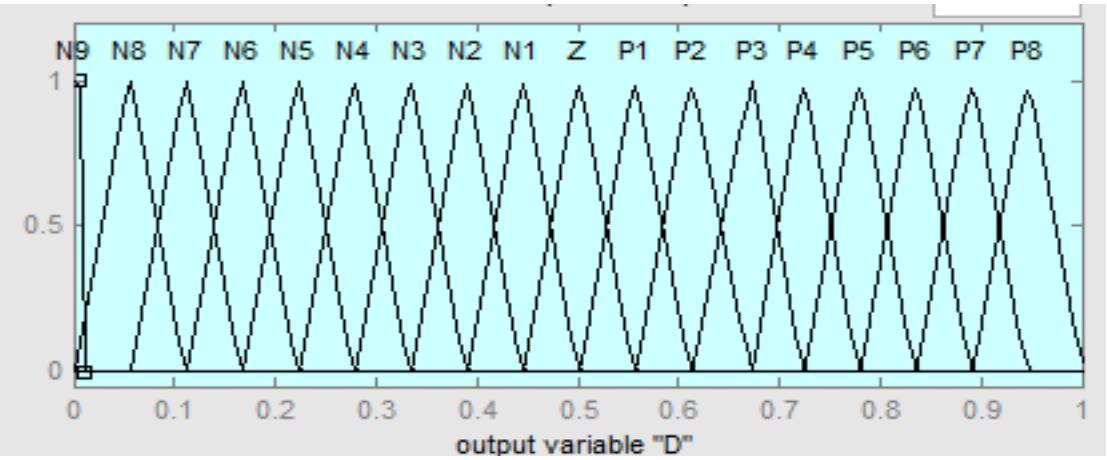

Fig. 8. Membership functions for Duty Ratio (D).

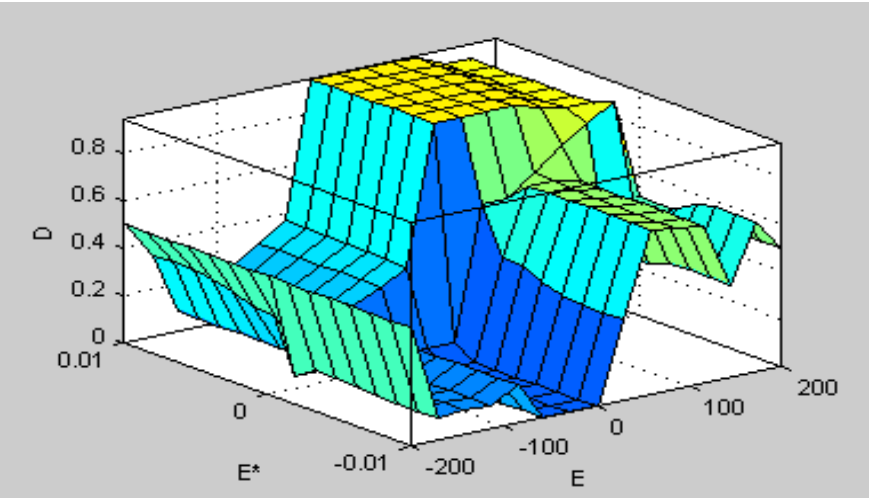

Fig. 9.Surface view of Rules of FLC.

V. SIMULATION DIAGRAMS

The proposed converter is simulated with PI and Fuzzy controller and their details are discussed

a)Proposed Converter with PI controller

International Journal of Environmental Sciences
ISSN: 2229-7359
Vol. 11 No. 19s, 2025
https://www.theaspd.com/ijes.php

Fig. 10 shows, A 24 V input voltage is fed to the converter, an output voltage of 398.3 V is obtained which is fed back as a feedback voltage to the PI controller; there it compares the feedback and the reference signal from which PWM pulse is generated which triggers the main switch of the converter.

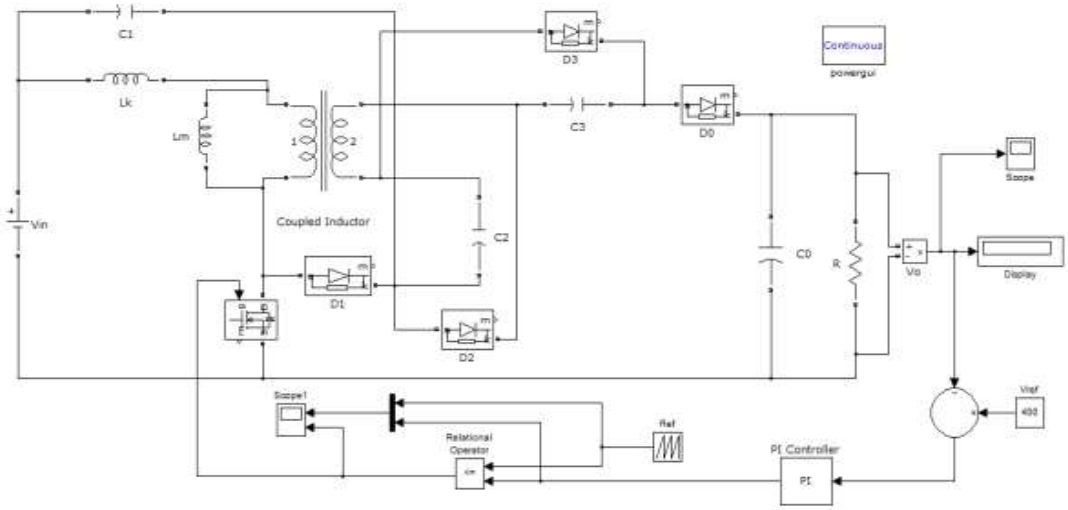

Fig. 10 Proposed Converter with PI controller.

b)Proposed Converter with FLC

In fig.11, for the same input voltage the converter is controlled by the newly designed FLC now 399.4 V output voltage is obtained.

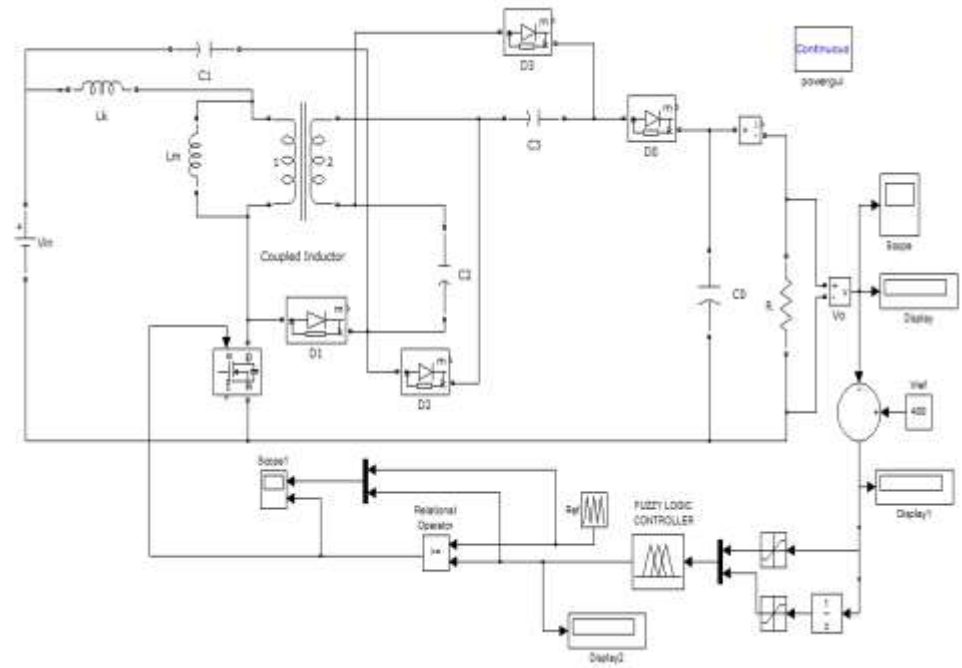

Fig. 11 Proposed Converter with FLC.

The output voltage from the converter is fed as feed back to the FLC; there it compares the feedback voltage signal and the reference voltage signal to produce PWM pulse which triggers the main switch of the converter. Thus the Voltage Drift problem is reduced using closed loop control of the proposed converter with FUZZY LOGIC CONTROLLER.

VI. SIMULATION RESULTS

a)Proposed converter with PI controller

Fig. 12. shows the simulation response of the converter with PI controller.

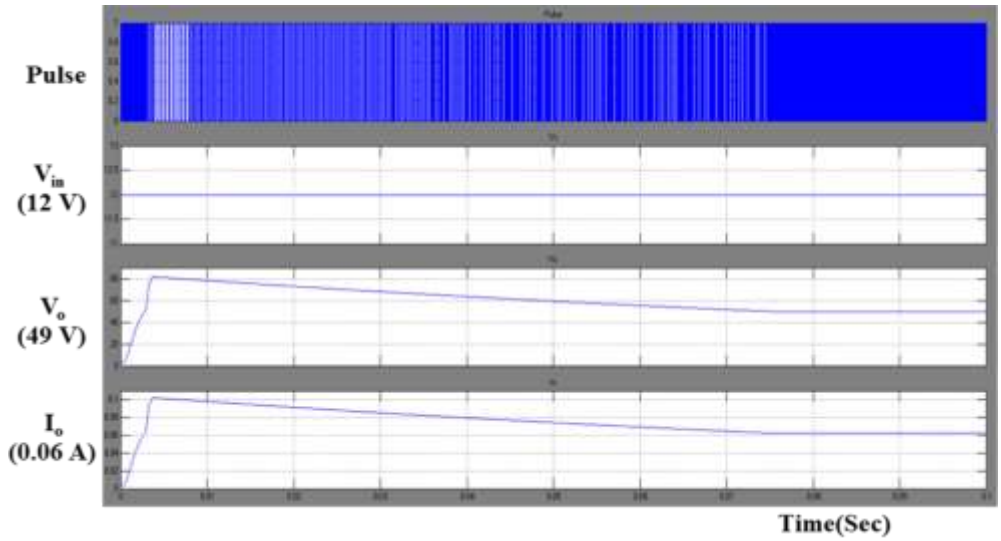

Fig.12 Pulse, Input Voltage,Output Voltage & Output Current (Vin = 24 V, V0 = 398.3 V & I0 = 0.5 A).

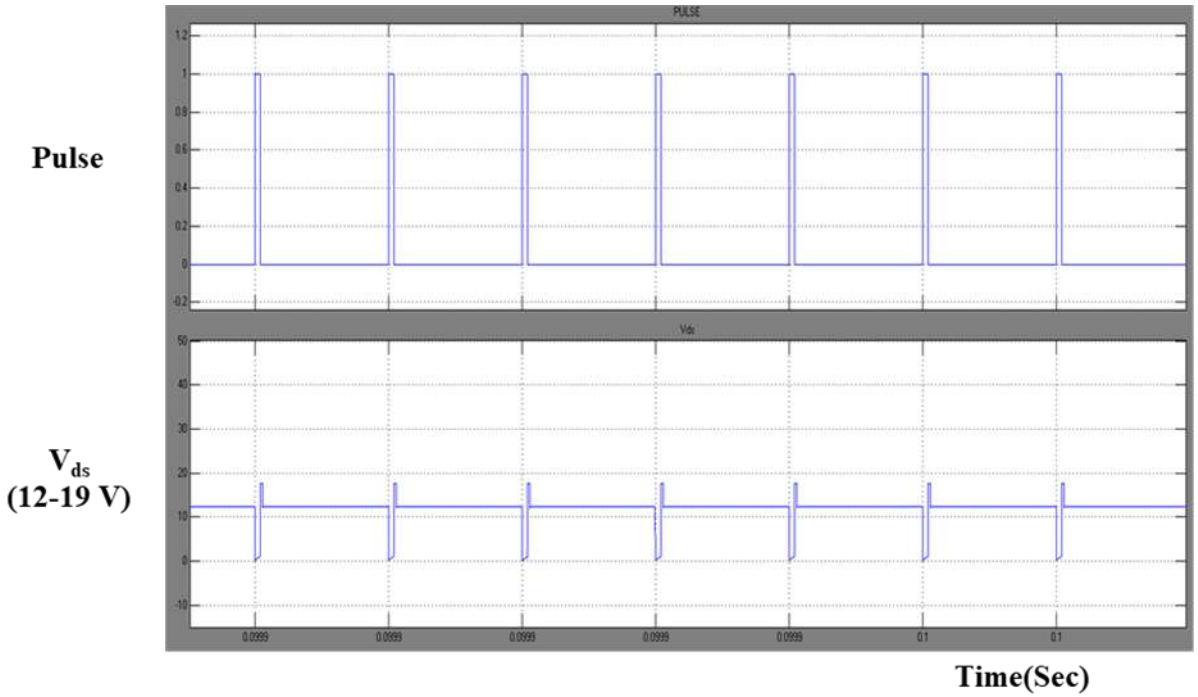

Fig. 13 Pulse, Voltage across Switch.

The switch voltage stress of the converter with PI controller is shown in fig.13

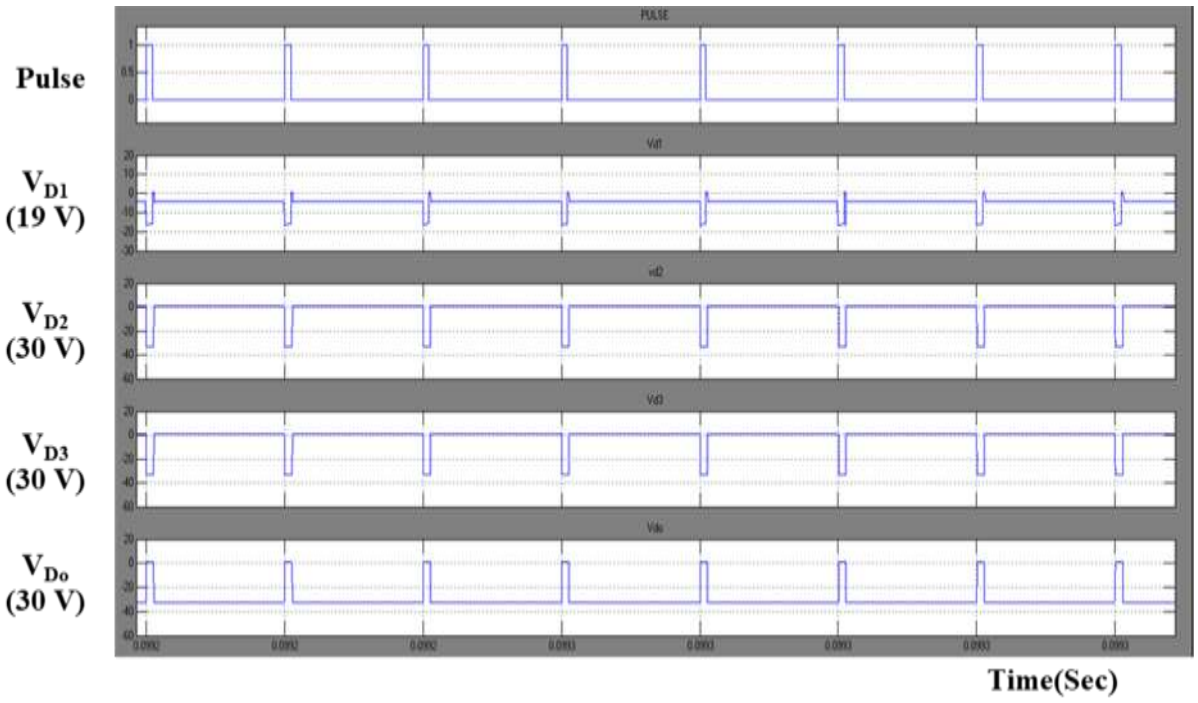

Fig.14 Pulse, Voltage across Diodes.

b)Proposed Converter with FLC

From fig. 15 it is clear that for the designed parameters, required output voltage and current is obtained. The duty ratio of the switch is adjusted by FLC to obtain the require output and also the voltage drift problem is

eliminated.

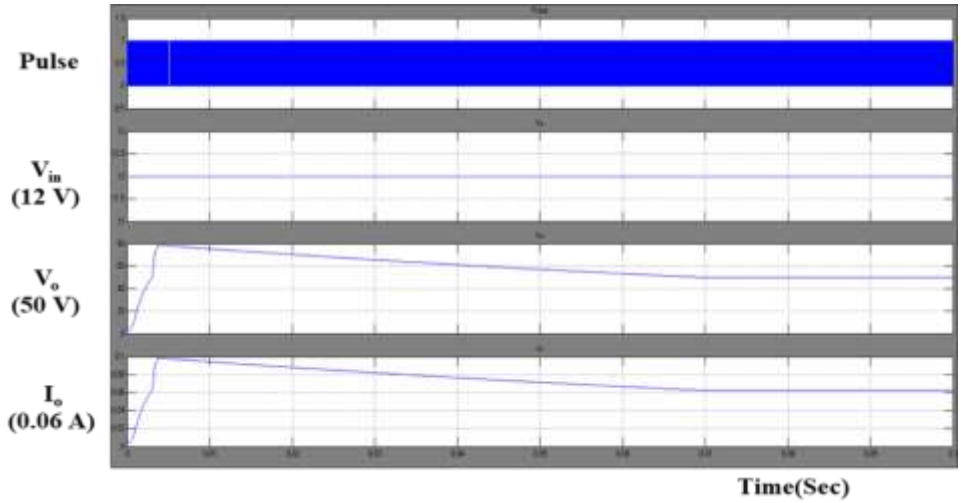

Fig. 15. Pulse, Input Voltage Output Voltage & Output Current

Further from fig. 16, the voltage stress of switch is much reduced than the circuit with PI controller.

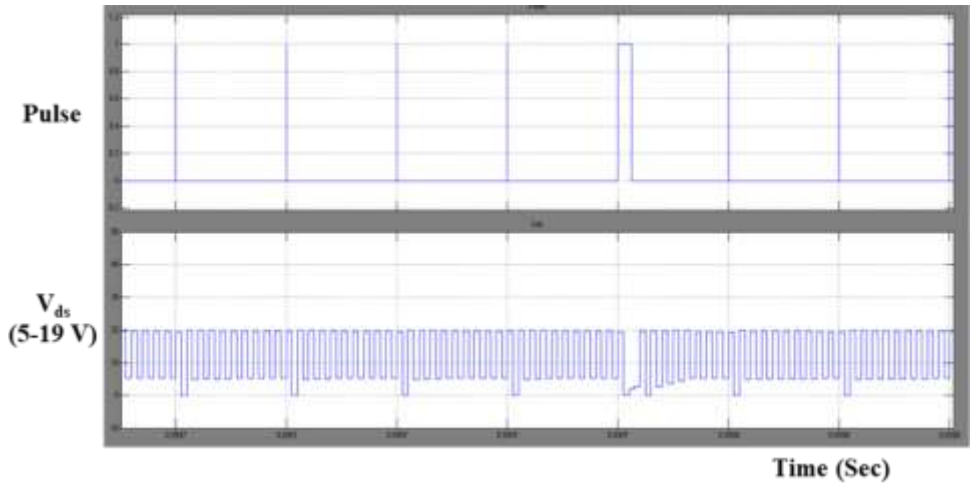

Fig. 16 Pulse, Voltage across Switch.

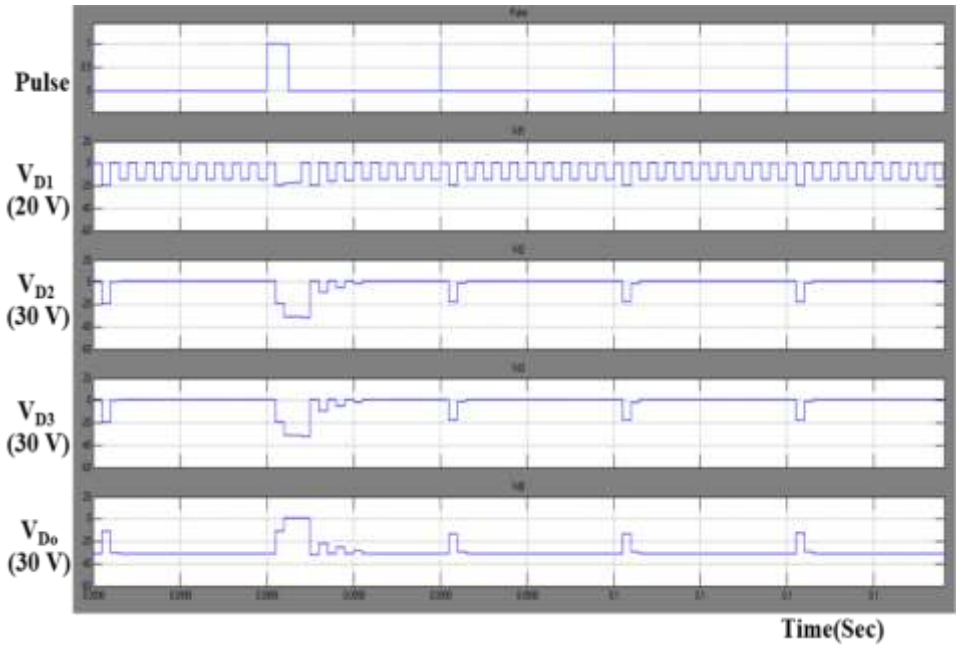

Fig. 17 Pulse, Voltage across Diodes.

From fig. 17, V_{D2}, V_{D3}, V_{D0} are equal and so, they are under the same voltage ratio, the voltage stresses can be adjusted by the turn ratio of the coupled inductor.

S.No	Type	Input Voltage (V)	Output Voltage (V)	Voltage Gain	Switch Voltage Stress (V)
1	Converter with PI controller	24	398.3	16.5	55-60
2	Converter with FLC	24	399.4	16.6	30-57

TABLE I1 Comparisons between Proposed Converter with PI Controller & FLC

S.No	Type	Input Voltage (V)	Output Voltage (V)	Voltage Gain	Switch Voltage Stress (V)
1	Converter with PI controller	12	49	16.5	12-19

2	Converter with FLC	12	50	16.6	5-19

VII. CONCLUSIONS

Here a high step-up dc–dc converter using coupled inductor with fuzzy logic control is simulated. By the capacitor charged in parallel and discharged in series by the coupled inductor, high step-up voltage gain is achieved. As the output voltage of the converter with FLC has minimum overshoot and produces a constant output current shows the better performance compared to the converter with PI controller.These studies could solve many types of problems regardless on stability because as we know that fuzzy logic controller is an intelligent controller to their appliances. Additionally, the switch voltage stress is reduced, thus a switch with low voltage ratings can be selected.

REFERENCES

[1] Maryam Hajilou;Hosein Farzanehfard;S. Ali Khajehoddin, "Nonisolated High Step-Up Impedance Source DC–DC Converter With ZVS Operation, Low Switches Voltage Stress, and Diodes Losses",IEEE ,Early Access Article, 2025
[2] T.F. Wu, Y.S. Lai, J.C. Hung and Y.M. Chen, —Boost Converter with Coupled Inductors and Buck–Boost Type of Active Clamp‖ IEEE Trans Ind. Electron.,vol. 55, no. 1, Jan. 2008.
[3] Junyan Hao;Minglei Zhang;Zijian Liu;Yanbo Zhang;Shubin Liu;Zhangming Zhu;Yan Zhu;Rui P. Martins;Chi-Hang Chan, "An Intrinsically PVT Robust 10-bit 2.6-GS/s Dynamic Pipelined ADC With Dual-Path Time-Assisted Residue Generation Scheme
[4] "IEEE Journal of Solid-State Circuits,Early Access Article, 2024
[5] J.M. Kwon and B.W. Kwon, —High Step-Up Active-Clamp Converter with Input-Current Doubler and Output-Voltage Doubler for Fuel Cell Power Systems‖, IEEE Trans. Power Electron., vol. 24, no. 1, Jan 2009.
[6] Borja Alberdi;Mikel Mazuela;Jon San-Sebastian;Roberto Sánchez;Asier Arruti;Iosu Aizpuru "Design and Validation of a Cost-Effective 300 W GaN-Based Step-Up Push-Pull Converter"IEEE Access, Vol.12, 2024.
[7] J. A. Carr, D. Hotz, J. C. Balda, A. Mantooth,A. Ong and A. Agarwal, —Assessing the Impact of SiC MOSFETs on Converter Interfaces for Distributed Energy Resources‖,IEEE Trans. Power Electron., vol. 24, no. 1, Jan 2009.
[8] G.S. Yang, T.J. Liang and J.F. Chen, —Transformerless DC–DC Converters With High Step-Up Voltage‖, IEEE Trans Ind. Electron., vol. 56, no. 8, Aug 2009.
[9] S.V. Araújo, R.P.T. Bascopé and G.V.T.Bascopé, —Highly Efficient High Step-Up Converter for Fuel-Cell Power Processing Based on Three-State Commutation Cell‖, IEEE Trans Ind. Electron., vol. 57, no. 6, June 2010.
[10] S.K. Changchien, T.J Liang, J.F. Chen and L.S. Yang, —Novel High Step-Up DC–DC Converter for Fuel Cell Energy Conversion System‖, IEEE Trans Ind. Electron., vol. 57, no. 6, June 2010.
[11] Y. Zhao, Y. Deng and Xiangning, —Interleaved Converter with Voltage Multiplier Cell for High Step-Up and High-Efficiency Conversion‖, IEEE Trans. Power Electron., vol. 25, no. 9, Sep 2010.
[12] J. Bauman and M. Kazerani, —A Novel Capacitor-Switched Regenerative Snubber for DC/DC Boost Converters‖, IEEE Trans Ind. Electron.,vol. 58, no. 2, Feb 2011.
[13] Y.P. Hsieh, J.F Chen, T.J Liangand L.S. Yang, —Novel High Step-Up DC–DC Converter with Coupled-Inductor and Switched-Capacitor Techniques for a Sustainable Energy System‖,IEEE Trans. Power Electron.,vol. 26, no. 12, Dec 2011.
[14] J.H. Lee, J.H. Park and J. H. Jeon, —Series-Connected Forward– Flyback Converter for High Step-Up Power Conversion‖, IEEE Trans. Power Electron.,vol. 26, no. 12, Dec 2011.
[15] Wuhua Li, Weichen Li, Xiangning He, David Xu and Bin Wu,
—General Derivation Law of Nonisolated High-Step-Up Interleaved Converters with Built-In Transformer‖, IEEE Trans Industrial Electron., Vol. 59, no. 3, Mar 2012.
[16] Amir Ramezani Roshnavand;Ebrahim Afjei "A Non-Isolated Coupled Inductor Soft Switched Step-Up DC–DC Converter With Reduced Voltage Stress on Semiconductors"IEEE Access,Vol.12,2024.
Tohid Nouri;Sara Hasanpour;Sze Sing Lee, "A Semiquadratic Trans-Inverse High Step-Up DC–DC Converter for Renewable Energy Applications"IEEE Transactions on Power Electronics,Vol.39,Issue 11,2024.